Structural Monitoring and Maintenance, *Vol. 10, No. 3 (2023) 243-260*
https://doi.org/10.12989/smm.2023.10.3.243

Seismic fragility analysis of base isolation reinforced concrete structure building considering performance – a case study for Indonesia

Faiz Sulthan *[1] and Matsutaro Seki[2]

[1]*Implementation Unit for Building Materials and Structures, Directorate General of Human Settlements, Ministry of Public Works and Housing, Panyawungan, Cileunyi, Bandung, West Java 40622, Indonesia*
[2]*Building Research Institute 1 Tatehara, Tsukuba, Ibaraki 305-0802, Japan*

(*Received August 17, 2023, Revised September 20, 2023, Accepted September 23, 2023*)

Abstract. Indonesia has had seismic codes for earthquake-resistant structures designs since 1970 and has been updated five times to the latest in 2019. In updating the Indonesian seismic codes, seismic hazard maps for design also update, and there are changes to the Peak Ground Acceleration (PGA). Indonesian seismic design uses the concept of building performance levels consisting of Immediate occupancy (IO), Life Safety (LS), and Collapse Prevention (CP). Related to this performance level, cases still found that buildings were damaged more than their performance targets after the earthquake. Based on the above issues, this study aims to analyze the performance of base isolation design on existing target buildings and analyze the seismic fragility for a case study in Indonesia. The target building is a prototype design 8-story medium-rise residential building using the reinforced concrete moment frame structure. Seismic fragility analysis uses Incremental Dynamic Analysis (IDA) with Nonlinear Time History Analysis (NLTHA) and eleven selected ground motions based on soil classification, magnitude, fault distance, and earthquake source mechanism. The comparison result of IDA shows a trend of significant performance improvement, with the same performance level target and risk category, the base isolation structure can be used at 1.46-3.20 times higher PGA than the fixed base structure. Then the fragility analysis results show that the fixed base structure has a safety margin of 30% and a base isolation structure of 62.5% from the PGA design. This result is useful for assessing existing buildings or considering a new building's performance.

Keywords: fragility curve; incremental dynamic analysis; performance level evaluation; seismic isolation

1. Introduction

As a country prone to earthquakes, Indonesia has had seismic codes for earthquake-resistant structures designs since 1970 and has been updated five times to the latest in 2019. In updating the Indonesian seismic codes, seismic hazard maps also update. There are changes to the Peak Ground Acceleration (PGA) values that can decrease or increase, caused by research developments related to hazard maps in Indonesia like the addition of newly identified active faults, revisions of the locations of previously known active fault traces, as well as improved estimates of maximum magnitudes and slip rates (Irsyam *et al.* 2017b, Nugroho *et al*. 2022). Under these conditions, an

*Corresponding author, Mr., E-mail: faiz.sulthan@pu.go.id

http://www.techno-press.org/?journal=smm&subpage=7 ISSN: 2288-6605 (Print), 2288-6613 (Online)

(a) (b)

Fig. 1 Post-earthquake damages (a) Hospital building in Palu Earthquake 2018 and (b) Residential building in Mamuju Earthquake 2021

analysis is needed to determine the effect of changing the earthquake's intensity on the structure's behavior. The analysis that can be used is seismic fragility analysis. This analysis can provide an overview of the structure's behavior towards damage limits with different earthquake intensities. It is useful for evaluating structures at various intensity values, such as PGA (Erberik 2015, Gautham and Krishna 2017, Rajkumari *et al.* 2022).

Several standards have been used as references in the history of the development of seismic codes in Indonesia. In 1970, Indonesian seismic codes referred to the Japanese standard, the New Zealand standard in 1983, Uniform Building Codes (UBC) in 2002, and then from 2012 until now, Indonesia consistently referred to U.S. standards, namely ASCE 7 (Kato *et al*. 2017, Nugroho *et al.* 2022). Based on referred of ASCE 7, Indonesian seismic design uses the concept of building performance levels consisting of Immediate occupancy (IO), Life Safety (LS), and Collapse Prevention (CP). In a linear design, the performance of the building was represented by an importance factor and risk category according to the occupancy of the building (ASCE, 2017a). Related to this performance, cases are still found in the field where buildings were damaged more after the earthquake than their performance targets, as an example in Figure 1. This problem often occurs due to issues with the poor quality of construction materials and workmanship (Pribadi *et al.* 2021). Based on investigations into post-earthquake damage in Indonesia, the poor quality of construction, especially the problem of detailing reinforcement, among others, is still found plain of rebars used, no shear rebar on beam-column joints, shear rebar that is not bent 135 degrees, and inadequate confinement rebar (Maidiawati *et al*. 2020).

In addition to problems related to building construction quality problems, performance targets that did not meet requirements have also happened due to earthquakes that occurred in more than one sequence. Such as mainshocks and aftershocks, which are close to occurring time and with relatively the same magnitude. Analysis of many post-earthquake cases showed that the risk of building collapse from cumulative aftershock damage must be considered (Augenti and Parisi 2010, Kossobokov and Nekrasova 2018). This phenomenon in Indonesia was the Mamuju Earthquake in 2021, where heavy damage or collapse resulted in offices, residential, and even hospitals after the aftershock (Supendi *et al.* 2021).

A seismic isolation system is one of the technologies that can be used to increase the building

performance level. Seismic isolation can make buildings have IO performance levels and resist aftershock sequences (Han *et al*. 2014, Zhai *et al*. 2016, Yenidogan 2021, Yang *et al.* 2023). In Indonesia, there have been several buildings built using this technology. In 2012 the first high-rise buildings in Indonesia to use seismic isolation were completed in 2012, a 26-story office building in the National Capital, Jakarta City, designed by local Indonesian firm Davy Sukamta & Partners (Sukamta 2014, Hussain *et al.* 2012). Until now, after more than ten years, even though the Indonesian seismic codes have regulated the procedures for designing it, the use of seismic isolation in Indonesia is still relatively small. One of the reasons is the common perception of unfavorable cost-benefit construction of seismic isolation compared to conventional fixed base buildings (Imran *et al*. 2021).

Regarding seismic fragility analysis, no study in Indonesia has researched this analysis on isolation systems. Seismic fragility analysis that has been investigated in Indonesia included non-engineered building housing by Khalfan (2013), Sarli *et al.* (2023), and fixed base reinforced concrete building by Muntafi *et al*. (2020), Juliafad and Gokon (2022), Irfan *et al*. (2022), Fauzan (2023). The previous studies focused on building structural systems primarily used in Indonesia, which are highly fragile to earthquakes. It is common knowledge that seismic isolation systems can improve building performance levels. Still, study on fragility analysis in Indonesia is needed to see the behavior of this system if the earthquake intensity increases much compared to the design earthquake intensity, and it can be a reference for the use of seismic isolation systems which are still few in Indonesia. Based on the background description, the main objective of this study is to analyze the seismic fragility of fixed base and base isolation structures designed with performance limit states (IO, LS, CP) against various PGA intensity values of 0.1-1.5 g based on Indonesia seismic hazard maps.

2. Methods

This study will focus on the target building for which the design is already available. From the existing design, then proceed with designing the isolation system without making any changes to the existing design. The target building was chosen because it is a typical design that is widely used and has a life safety performance target that is still possible to improve. The seismic isolation design acceptance criteria in this study refer to SNI 1726:2019 and the Japanese Standard. After the seismic isolation design is obtained, Incremental Dynamic Analysis (IDA) with Nonlinear Time History Analysis (NLTHA) is carried out on the existing target building design and the newly obtained seismic isolation design.

2.1 Target building

The target building is a prototype design 8-story medium-rise residential building. Prototype design is a term for a design that is used as a typical design for construction in several areas with the same seismic hazard level. In this case, a prototype design used as a target building is a residential building for a high seismicity area by the Indonesian Ministry of Public Works and Housing. Target building structure drawing and technical information can be shown in Fig. 3, Table 1, and Fig. 4.

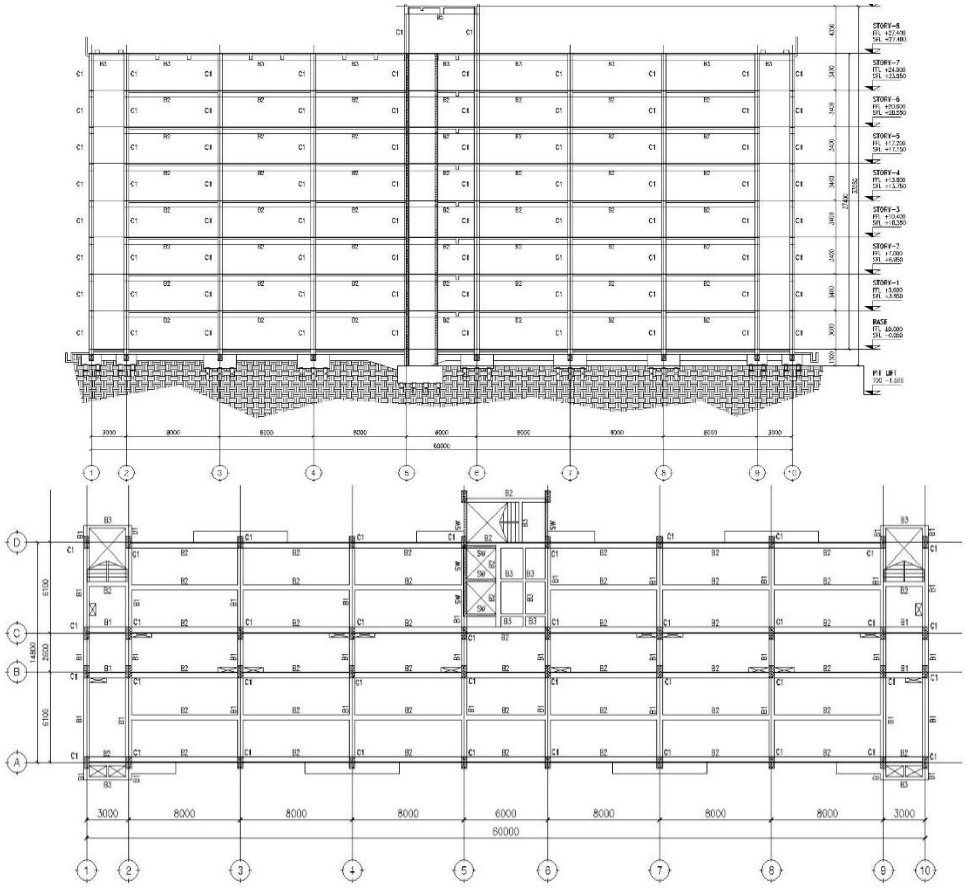

Fig. 2 Target building structure drawing

Table 1 Target building information

Parameters	Information
Occupancy	Residential
Structure system	Special moment frame reinforced concrete with shear wall
Number of stories	8 stories
Total height	27.4 m
Risk category	II
Seismic importance factor	1.0
Site Class	D
Building codes	Indonesian Seismic Codes (SNI 1726:2019)
Seismic parameters design	$\boldsymbol{S_{DS}}$ = 1.00 g; $\boldsymbol{S_{D1}}$ = 0.68 g
Concrete strength (f_c')	30 MPa (Beam and slab); 35 MPa (Column and Shear wall)
Yield strength of rebar (f_y)	420 MPa (main and hoops)
Number of type members	Column type = 1; Beam type = 5; Shear wall type = 1; Slab type = 1

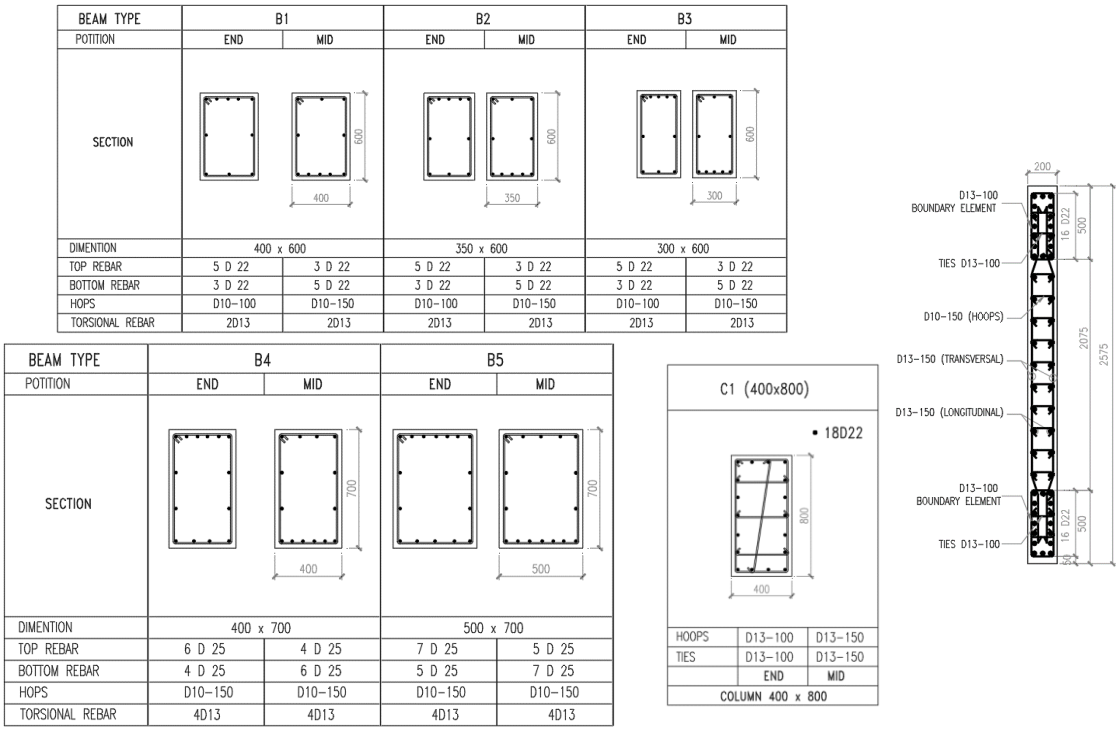

Fig. 3 Target building structure member's detail

2.2 Base isolation design

Seismic isolation design is carried out on target building designs without changing the structural design. The target building structures have been designed with seismic codes so that some design parameters can be used, such as the total building mass and base shear coefficient. The type of isolation used is Bridgestone (2017) products, where the products have been tested and used globally, especially in Indonesia. In this study, three types of isolators were used, namely natural rubber bearing (NRB), lead rubber bearing (LRB), and sliding rubber bearing (SRB).

The parameters used in seismic isolation design are base shear coefficient (α_1), natural periods (T_f), shear coefficient of the damper (α_s), and design displacement of the seismic isolation system (D_d). The base shear coefficient is a parameter related to the design seismic force intensity used, a base shear coefficient of 0.1 is obtained. The natural period (T_f) is calculated using Eq. (1), design displacement (D_d) can use the formula from the Indonesian standard in Eq. (2), and the shear coefficient of the damper (α_s) can be calculated using Eq. (3).

$$T_f = 2\pi\sqrt{\frac{m}{K_f}} \tag{1}$$

Where m is the total mass of the building, and K_f is the stiffness of the seismic isolation system. The total structural mass of the upper structure is 8774.14 tons.

Table 2 The general value of seismic isolation design parameters in Japan (JSSI, 2010)

Design parameters	General value in Japan
Base shear coefficient (α_1)	0.05 – 0.20
Design displacement (D_d)	30 – 50 cm
Natural periods (T_f)	3 – 5 s
Shear coefficient of damper (α_s)	0.02 – 0.10

Table 3 Design parameter result

Design parameters	General value	Design result	Status
Base shear coefficient ($\boldsymbol{\alpha_1}$)	0.05 – 0.20	0.1	OK
Design displacement ($\boldsymbol{D_d}$)	30 – 50 cm	39 cm	OK
Natural periods ($\boldsymbol{T_f}$)	3 – 5 s	3.5 s	OK
Shear coefficient of damper ($\boldsymbol{\alpha_s}$)	0.02 – 0.10	0.02	OK
Wind load ($\boldsymbol{F_w}$) < characteristic shear strength ($\boldsymbol{Q_y}$)	> 1265.88 kN	1717.6 kN	OK

$$D_d = \frac{gS_{D1}T_f}{4\pi^2 B_D} \tag{2}$$

Where S_{D1} is design spectral acceleration at a period of 1, and B_D is the damping coefficient related to effective damping (β).

$$\alpha_s = \frac{Q_y}{mg} \tag{3}$$

The Japan Society of Seismic Isolation (JSSI) has a range of values for seismic isolation design parameters as shown in Table 2, where these values are the ideal values of a design such as the value of the shear coefficient of damper (α_s), where if it is large, the response reduction effect of the upper structure will be weakened, and if it is too small, the response displacement increases.

In addition to the design parameter values discussed earlier, there are also force requirements governing stability such as the wind load (F_{wind}) which must be lower than the characteristic shear strength (Q_y) as Eq. (4). In the target building design, the design wind load is 1265.88 kN.

$$F_{wind} < Q_y \tag{4}$$

By calculating the service load (dead load, superimposed dead load, live load, wind load, and earthquake load) following Indonesia codes (SNI 1726:2019) and design parameters following Japanese standards (JSSI, 2010), the results of the seismic isolation design can be seen in Fig. 5 and Table 3 for the design parameters.

Referring to the catalog of Bridgestone (2017), the nonlinear properties of the seismic isolation type used can be seen in Table 4.

Furthermore, in the IDA analysis, the earthquake's intensity will be greater than the design earthquake, so in the isolation system, displacements will exceed the design displacements. In the building design plan, there is a retaining wall around the isolation system, the distance between the seismic isolation system and the retaining wall is determined at shear strain (γ) 300% of the height

Table 4 Properties of isolator type (Bridgestone 2017)

Characteristics	Isolator type			
	LL070G4-E	LL065G4-E	NH060G4	SL050GC
Diameter (mm)	700	650	600	500
Total height (mm)	324.9	330.4	407.9	122.8
Lead plug diameter (mm)	100	90	-	-
Total rubber thickness (mm)	167	162	200	60
Displacement at shear strain (γ) 300% (mm)	501	486	600	-
Compression stiffness (kN/m)	2680	2400	1370	3290
Nominal long-term compression load (kN)	4310	3410	1700	1960
Shear initial stiffness (kN/m)	11700	10300	-	3850
Shear equivalent stiffness (kN/m)	1270	1100	554	-
Shear post-yield stiffness (kN/m)	899	792	-	-
Shear yield strength (kN)	62.6	50.7	-	-
Damping ratio	0.181	0.174	-	-

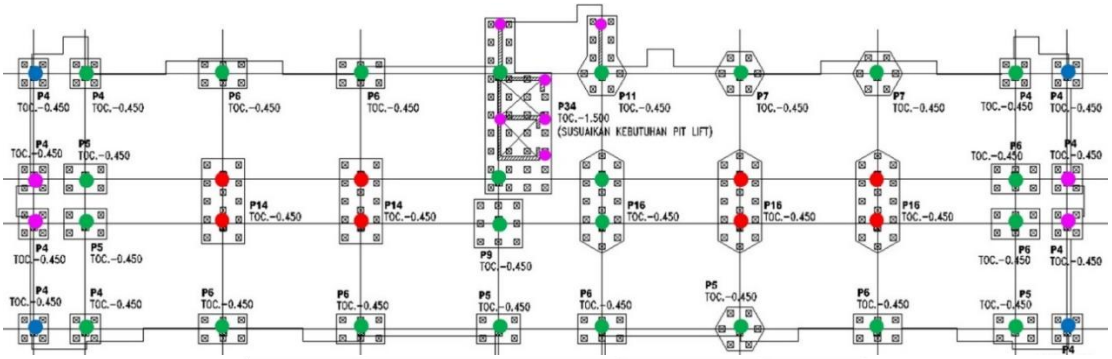

Legend	Type	Type code	*Number*
●	Lead Rubber Bearing	LL070G4-E	8
●	Lead Rubber Bearing	LL065G4-E	24
●	Natural Rubber Bearing	NH060G4	4
●	Elastic Sliding Bearing	SL050GC	10
Total			46

Fig. 4 Design of base isolation

of the total rubber thickness. This value is the assumption of rubber conditions that have not yet been broken and are still performing quite well, as shown in Fig. 5. The value of total layer displacement for each type of seismic isolation system is also obtained from the product catalog, which can be seen in Table 4.

Based on the displacement conditions at shear strain (γ) 300% in Table 4, the gap between the seismic isolation system and the retaining wall is 500 mm. This gap in the analysis is modeled as a

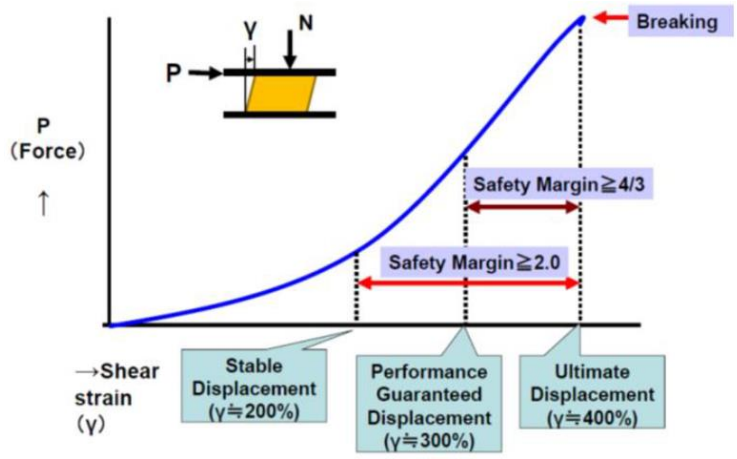

Fig. 5 Isolator displacement condition in shear strain (Seki and Lee 2022).

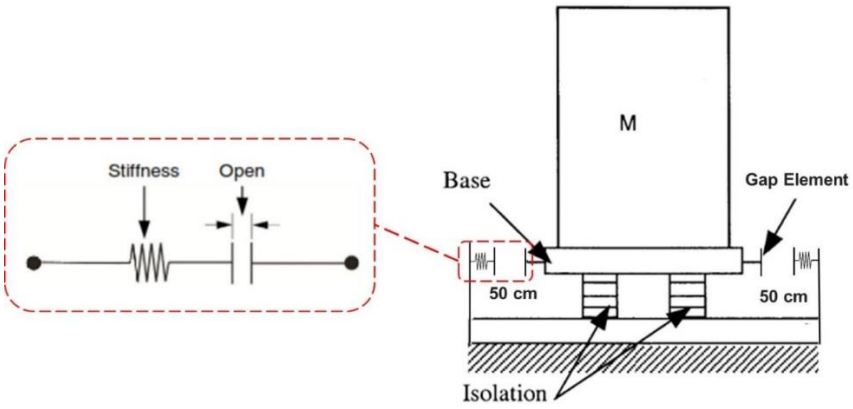

Fig. 6 Concept of seismic gap element model for pounding effect

gap element. The gap element is a type of model link/spring, which is compression-only. A compression gap is not activated until the isolation displacement reaches the seismic gap (open). The defined stiffness only effects when the deformation exceeds the defined seismic gap, as shown in Fig. 6.

Many studies have suggested various assumptions for assigning stiffness to the seismic gap element. This study uses stiffness value based on experimental test results by Miwada *et al*. (2012), who tested a reinforced concrete retaining wall 200 mm thick and 1.2 m high. In the test, the upper structures were pulled the measured stiffness of the retaining wall was 104600 kN/m (104.6 kN/mm). Qu *et al.* (2013) also used the stiffness retaining wall results in their study.

2.3 Selected ground motion

Based on SNI 1726:2019 regulations to carry out NLTHA, a minimum number of ground motions is required of eleven. The eleven ground motions were selected referring to Indonesian

Table 5 Selected ground motion

Number	Event	Earthquake Type	Code Station	Magnitude	Radius (km)
1	Kobe (1995)	Inland	(AMA)	6.9	11.34
2	Superstition Hills-02 (1987)	Inland	(WSM)	6.54	13.52
3	Northridge (1994)	Inland	(WIL)	6.69	23.07
4	Kocaeli (1999)	Inland	(DZC)	7.5	13.6
5	Landers (1992)	Inland	(PSA)	7.28	36.15
6	Loma Prieta (1989)	Inland	(GR2)	6.93	10.38
7	Tohoku (2011)	Subduction	(MYG015)	9	137
8	Mentawai (2007)	Subduction	CTO Station PSKI	7.9	167.7
9	Chile (2010)	Subduction	(CCSP)	8.8	109.1
10	Tokachi-OKI (2003)	Subduction	(HKD098)	8	88.4
11	El Salvador (2001)	Subduction	CIG station SM	7.7	79.7

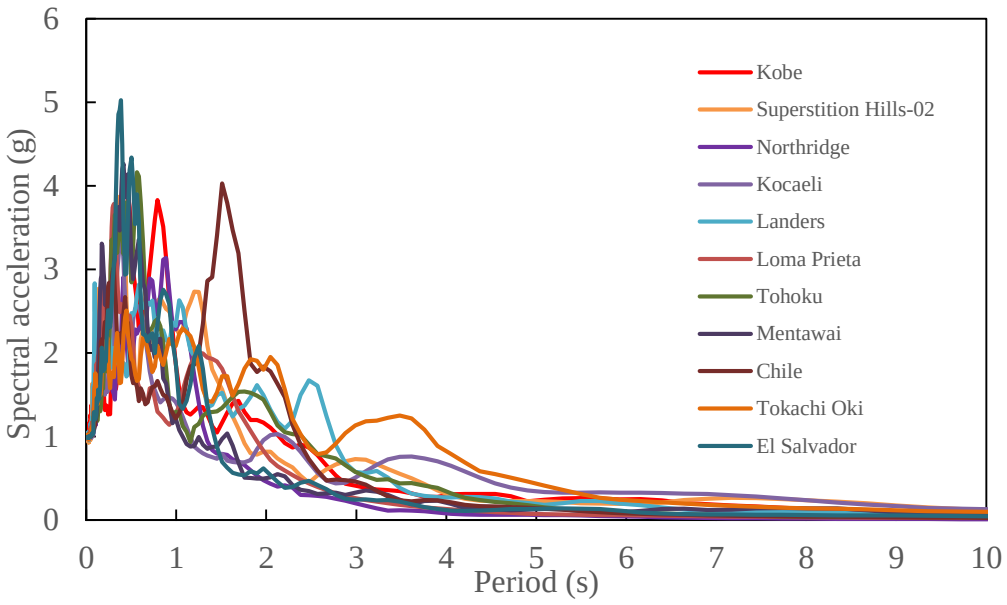

Fig. 7 Selected ground motion scaled at PGA of 1.0 g

deaggregation maps data which explains the source magnitude (M) and distance (R) for each earthquake source mechanism and soil classification map (National Center for Earthquake Studies, 2022, Irsyam *et al*. 2017a), 11 ground motions were chosen for analysis, as shown in Table 5. This ground motion data is obtained from the Pacific Earthquake Engineering Research Center (PEER) database for inland earthquakes and the Center for Engineering Strong Motion Data (CESMD) database for subduction earthquakes.

2.4 Incremental dynamic analysis

Incremental Dynamic Analysis in this study uses the NLTHA principle, carried out on several intensity measurements in the form of PGA. The PGA interval used is 0.1 - 1.5 g. This value is based on Indonesian seismic hazard maps in that range. For damage measurement in the form of inter-story drift ratio maximum (IDR_{max}) which is referring to performance level IO, LS, and CP. In this study, the seismic fragility performance level limits use global criteria based on inter-story drift constraints. A pushover analysis is carried out to determine the capacity and mechanism of plastic hinges at each drift limit. The results of the pushover analysis on the target building show that the lateral capacity of the X-direction is smaller than the Y-direction, and the plastic hinge results are the basis for determining the limits of IDR used in this study at each performance level, namely IO of 1.0%, LS of 2.0%, and CP of 2.5%. This CP limit slightly differs from ASCE 41-17 (ASCE, 2017b), which uses 4.0%. The reason is that when the structure gets the IDR range of 2.5-3%, plastic hinge occurs with criteria exceeding CP, so by still considering the performance level acceptance criteria for the element and for conservative, it was decided to limit the CP of 2.5%. This limitation is also used by Xue *et al*. (2008) and another study by Ibrahim and El-Shami (2011).

Furthermore, the resulting IDA from 11 ground motions can be evaluated to be the logarithm of the median data, $\ln(IDR_{max})^{50\%}$ and the equivalent dispersion, δ_{eq} of data to be used as a parameter for the lognormal distribution. Benjamin and Cornell (1970) said that the equivalent dispersion, δ_{eq} is approximately equal to the coefficient of variation of the data, which can be calculated by Eq. (5).

$$\delta_{eq} = \frac{\ln(IDR_{max})^{84\%} - \ln(IDR_{max})^{16\%}}{2} \tag{5}$$

Using the formula from Nagae *et al*. (2006), the probability of the IDR_{max} exceedance against the idr limit of each performance level can be calculated by Eq. (6).

$$P[IDR_{max} > idr] = 1 - P[IDR_{max} \leq idr] = 1 - \Phi\left(\frac{\ln(idr) - \ln(IDR_{max})^{50\%}}{\delta_{eq}}\right) \tag{6}$$

IDA is only carried out in the direction of the weak direction of the building, in this case, the X-direction, because in this study, the structure is modeled in full three dimensions, IDA will take a lot of time to use 11 ground motions and do it on a fixed base and base isolation. Then the analysis of the weak axis has also been deemed sufficient to represent the worst possible conditions.

3. Result and discusion

The results of the IDA curve showing the relationship between the intensity measure (PGA) and the damage measure (IDR_{max}) can be seen in Figs. 8 to 9. In this paper, for each Figure that contains 11 ground motions, the colors of the lines were made the same as representing each ground motion to make it easier to read. The IDA curve results of the fixed base structure in Figure 8 show the results for each ground motion are various. This is in accordance with what was expected because the selection of ground motion was also made by considering different characteristics. Ground motion which gives a greater IDR_{max} result was Chile, and the lowest was Northridge. A fixed based structure's natural period was around 1.0-1.5 s. By looking at the

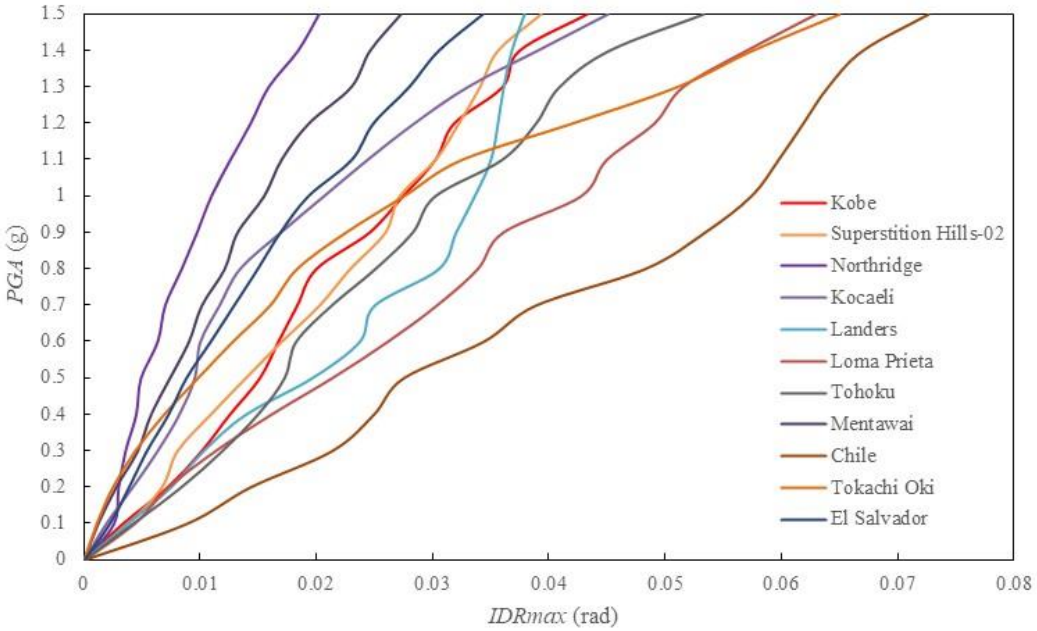

Fig. 8 IDA curve of the fixed base structure

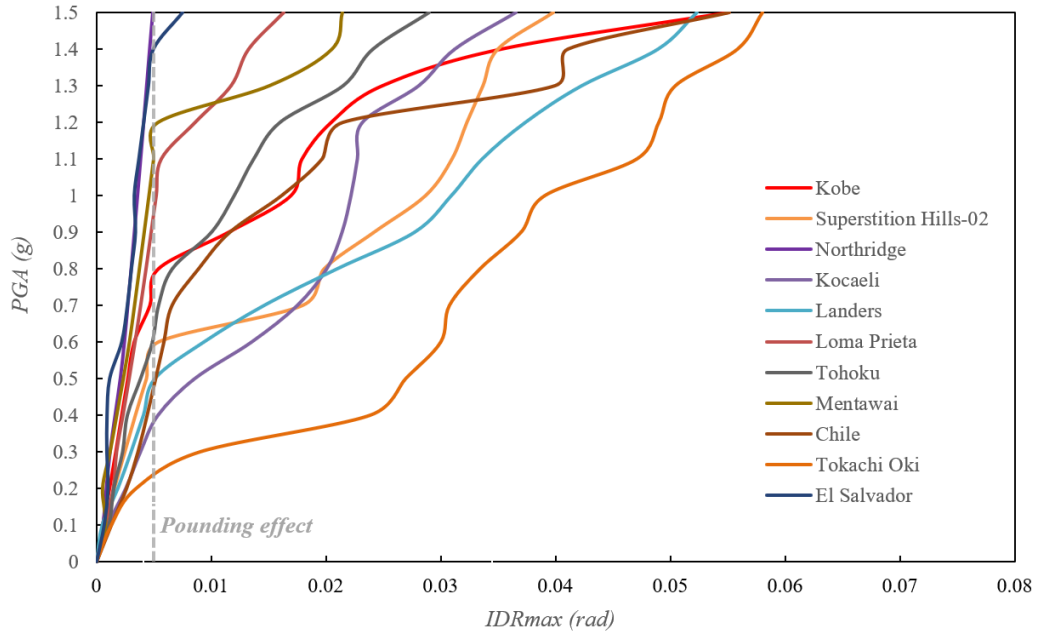

Fig. 9 IDA curve of the base isolation structure

dominant period of ground motion in Fig. 7, it can be understood that the ground motion response gives the greatest and lowest damage.

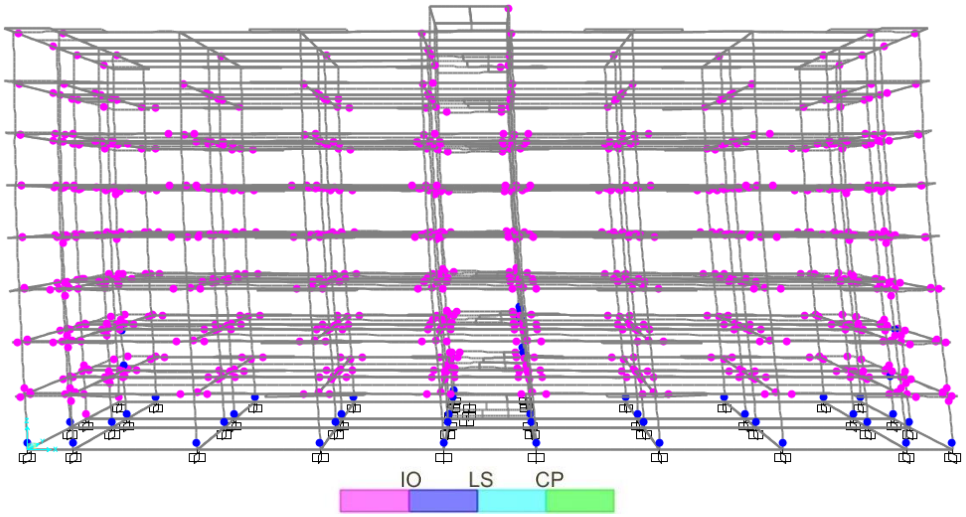

Fig. 10 Plastic hinges result using the Kobe Earthquake scaled at PGA of 0.4 g of fixed base structure

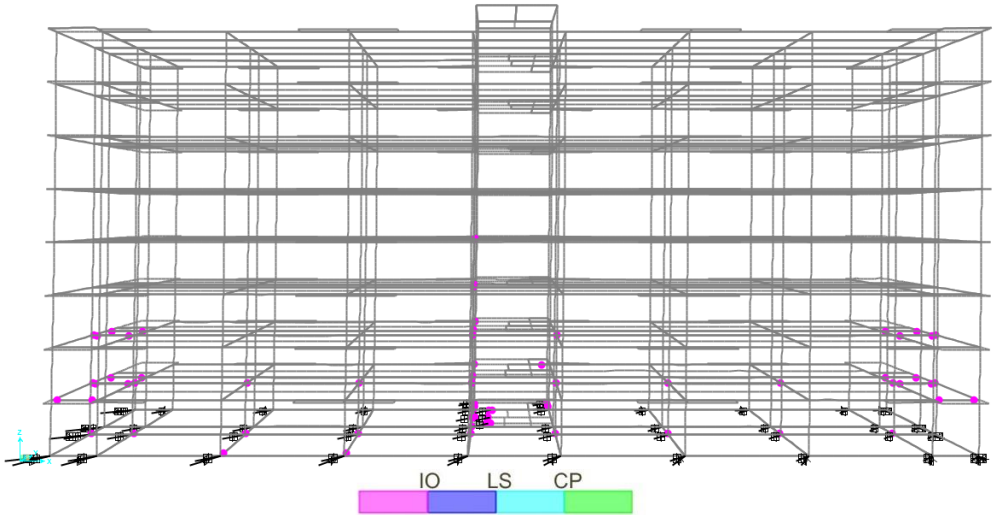

Fig. 11 Plastic hinges result using the Kobe Earthquake scaled at PGA of 0.4 g of base isolation structure

The IDA curve of the base isolation structure in Fig. 9 shows a smaller IDR result than a fixed base structure. As known, the base isolation provides better performance. Still, in an earthquake that causes a displacement of the isolation system that is greater than the seismic gap of 50 cm, the isolation system will have a pounding effect and cause the upper structures to begin to experience damage. This pounding effect can be seen in lines that intersect the gray dotted line. The magnitude of the PGA that causes this effect is also different for each ground motion, depending on the dominant period of the ground motion. Fig. 7 shows each ground motion's dominant period,

Table 6 Statistical evaluations of IDA result

PGA	Fixed base structure				Base isolation structure			
	16^{th}	50^{th}	84^{th}	δ_{eq}	16^{th}	50^{th}	84^{th}	δ_{eq}
0.1	0.0012	0.0033	0.0047	0.6880	0.0005	0.0008	0.0013	0.4522
0.2	0.0027	0.0067	0.0088	0.5873	0.0008	0.0015	0.0027	0.5932
0.3	0.0043	0.0080	0.0126	0.5376	0.0011	0.0023	0.0042	0.6540
0.4	0.0056	0.0109	0.0168	0.5455	0.0016	0.0027	0.0068	0.7392
0.5	0.0072	0.0139	0.0218	0.5569	0.0020	0.0038	0.0100	0.8079
0.6	0.0088	0.0167	0.0268	0.5569	0.0024	0.0049	0.0148	0.9095
0.7	0.0099	0.0183	0.0310	0.5731	0.0027	0.0054	0.0190	0.9722
0.8	0.0118	0.0200	0.0350	0.5447	0.0030	0.0066	0.0220	0.9879
0.9	0.0129	0.0245	0.0374	0.5326	0.0034	0.0115	0.0285	1.0630
1	0.0151	0.0274	0.0439	0.5338	0.0035	0.0161	0.0316	1.0929
1.1	0.0166	0.0302	0.0462	0.5110	0.0038	0.0179	0.0347	1.1018
1.2	0.0189	0.0322	0.0501	0.4872	0.0041	0.0205	0.0383	1.1144
1.3	0.0224	0.0360	0.0525	0.4263	0.0045	0.0249	0.0429	1.1244
1.4	0.0241	0.0374	0.0583	0.4415	0.0050	0.0312	0.0495	1.1510
1.5	0.0267	0.0433	0.0656	0.4500	0.0073	0.0366	0.0553	1.0110

Table 7 Lognormal distribution parameter for fragility curve

Performance level	IO (1.0% = 0.010 rad)		LS (2.0% = 0.020 rad)		CP (2.5% = 0.025 rad)	
Parameters	μ	σ	μ	σ	μ	σ
Fixed base	-1.4325	0.6207	-0.3103	0.5055	-0.0970	0.4877
Base isolation	-0.1232	0.4365	0.1548	0.4319	0.2436	0.4319

and the base isolation structure has a natural period of 3.5 s. In that period, Tokachi-Oki ground motion gives the most significant damage, and Northridge has the lowest response as in the IDA curve. As an example of the analysis results, Figs. 10 and 11 show the plastic hinges in fixed base and base isolation structural systems.

Using the Kobe earthquake ground motion scaled at PGA of 0.4 g sample, several plastic hinges with the LS category are occurring in a fixed structure, this result is in accordance with the results of the IDR in Fig. 8. In the base isolation structure, the upper structure is deformed like a rigid body with a small IDR, making very few occurrences of plastic hinges, and their categories are also still IO.

The results of the IDA curves on the fixed base and base isolation structure are then evaluated statistically by calculating the 16th, 50th, and 84th percentile to obtain the median and equivalent dispersion (δ_{eq}) values for each PGA intensity. Table 6 shows the results of the statistical calculations.

The results of the statistical evaluation show that the IDA result is quite varied, indicated by the equivalent dispersion (δ_{eq}) value, this shows that 11 ground motions give a varied response to the structure. The dotted horizontal line shows each performance level limit, which was then calculated with the probability of exceedance using Eq. (22). Furthermore, the results were

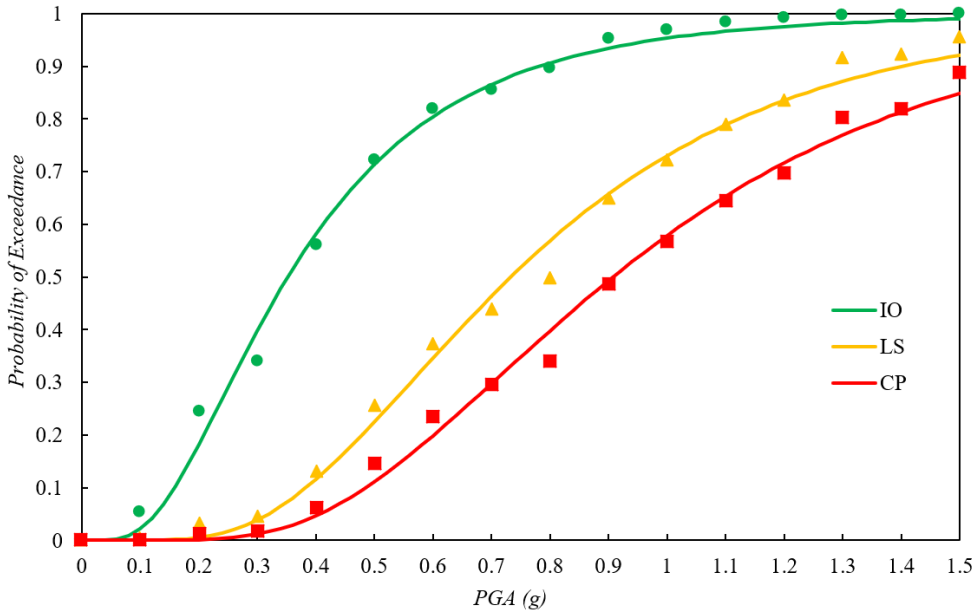

Fig. 12 Fragility curve of the fixed base structure

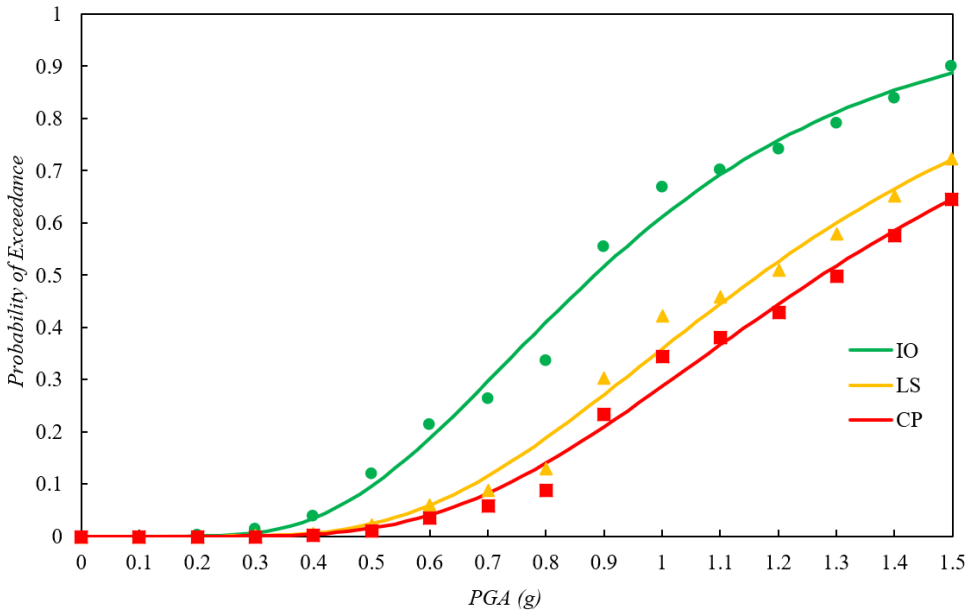

Fig. 13 Fragility curve of the base isolation structure

calculated for the lognormal distribution parameters such as the mean (μ) and standards deviation (σ) to obtain the fragility curve. The results of calculating the lognormal distribution parameter can be seen in Table 7.

Table 8 PGA values range of performance levels at target reliability

Risk Category	Occupancy (SNI 1726:2019)	POE (ASCE 7-16)	PGA limit					
			Fixed base structure			Base isolation structure		
			IO	LS	CP	IO	LS	CP
I-II	Residential Office Factory	25 %	≤0.23 g	>0.23 g ≤0.52 g	>0.52 g ≤0.65 g	≤0.65 g	>0.65 g ≤0.87 g	>0.87 g ≤0.95 g
III	Prison Meeting hall Sport Centre	15 %	≤0.18 g	>0.18 g ≤0.43 g	>0.43 g ≤0.54 g	≤0.56 g	>0.56 g ≤0.75 g	>0.75 g ≤0.81 g
IV	Hospital School Disaster shelter	9 %	≤0.15 g	>0.15 g ≤0.37 g	>0.37 g ≤0.47 g	≤0.48 g	>0.48 g ≤0.65 g	>0.65 g ≤0.70 g

Table 9 PGA limit ratio of the base isolation to the fixed base structure

Risk Category	PGA limit ratio of the base isolation to the fixed structure		
	IO	LS	CP
I-II	2.80	1.67	1.46
III	3.11	1.74	1.50
IV	3.20	1.76	1.49

The fragility curve in Figs. 12 and 13 shows the relationship of the Probability of Exceedance (POE) at each performance level in the PGA range of 0.1-1.5 g. POE is the probability that IDR_{max} exceeds the limit for each performance level (IO of 1.0%, LS of 2.0%, and CP of 2.5%). With a simple observation, we can compare the results of the fragility curve, which shows that the base isolation structure has a very significant increase compared to the fixed base structure. For a more detailed analysis, the desired reliability target was required.

Referring to ASCE (2017a), a reliability target is determined based on the building risk category. Target reliability can also be called target probability of failure or probability of exceedance (POE) in this paper. This target was determined based on a detailed seismic fragility analysis study by FEMA (2009). The building risk category has a relationship with this target value because the building risk category shows the level of building risk according to its occupancy, where the higher the risk of a building such as a hospital or nuclear facility, the smaller the POE target. The classification of risk targets based on occupancy is determined by the government in seismic codes, in this case, the Indonesian government in SNI 1726:2019. The relationship, risk category, occupancy, POE targets, and PGA value at target reliability from fragility curves result as shown in Table 8.

Table 8 can explain the performance level of the target building at several PGA levels. The target building in this study was designed using DBE (2/3 MCER) PGA = 0.40 g with risk category II. Referring to the results in Table 8, the performance was LS for a fixed structure and IO for an base isolation structure. Comparing the PGA limit value on each target reliability and risk category shows how significant the use of base isolation structure is, which can be used on PGA larger than fixed base structures with a ratio of 1.46-3.20, as shown in Table 9.

These results can also indicate the safety margin level of the design result. Fixed base and base isolation structures were designed with different performance targets. The fixed base was designed with LS targets and base isolation with IO targets. Used limit values for each performance target, the safety margin for the fixed base structure is 0.52 g / 0.40 g = 1.3 (30%), and the base isolation structure is 0.65 g / 0.40 g = 1.625 (62.5%). These results are very valuable which can be used to determine the performance level of existing buildings if the PGA value increases in the future.

4. Conclusions

This study focused on analyzing the base isolation systems for target building and then performing seismic fragility for a case study in Indonesia. Based on the analysis of the results that have been carried out, the following are the points of conclusion in this study:

- The design results using a base isolation system show increased performance in the target building. Target buildings with a performance level of LS can increase to IO, a comparison of IDA results shows a trend of significant performance improvement, with the same performance level target and risk category, base isolation can be used at 1.46-3.20 times higher PGA than the fixed base structure.
- The results of fragility analysis using IDA are very effective for seeing the fragility and reliability of the response structure. For fragility, the results are that the fixed base structure has a safety margin of 30% and a base isolation structure of 62.5% from the PGA design. The safety margin is the range of structural performance targets still being achieved before the performance target decreases.

The study provides a fragility curve explaining the probability of structure performance levels at different PGA intensities. The fragility curve is very useful for assessing fixed base buildings that have been built or considering new buildings using a seismic isolation system. These results are also expected to be helpful as a reference for the use of seismic isolation systems in Indonesia, which are still rare, but it is hoped that their use will increase in the future.

Acknowledgments

Thanks to the Building Research Institute, Ministry of Land Infrastructure and Transport (MLIT), Japan, this study can be carried out thanks to the help where the first author conducted his research.

References

American Society of Civil Engineers (ASCE). (2017a), ASCE 7-16 Minimum design loads and associated criteria for buildings and other structures. Virginia, United States: American Society of Civil Engineers. ASCE/SEI 7-16. https://doi:10.1061/9780784414248.

Augenti, N. and Parisi, F. (2010), “Learning from construction failures due to the 2009 L'Aquila, Italy, earthquake”, *J. Perform. Constr. Fac.*, **24**(6), 536-555. https://doi.org/10.1061/(ASCE)cf.1943-5509.0000122.

Benjamin, J.R. and Cornell, C.A. (1970), Probabilty statistics and decision for civil engineers. McGraw-Hill,

Inc., New York.
Bridgestone. (2017), Bridgestone seismic isolation product line-up (catalog), Bridgestone.
Erberik, M.A. (2015), "Seismic fragility analysis", *Encyclopedia Earthq. Eng.*, 1-10. https://doi.org/10.1007/978-3-642-36197-5_387-1.
Fauzan, Kurniawan, R., Syahdiza, N., Al Jauhari, Z. and Nugraha, M.D.A. (2023), "Fragility curve of school building in Padang City with and without retrofitting due to earthquake and tsunami loads", *Int. J. Geomate*, **24**(101). https://doi.org/10.21660/2023.101.g12251.
Gautham, A. and Krishna, K.G. (2017), "Fragility analysis – a tool to assess seismic performance of structural systems", *Materials Today Proceedings*, **4**(9), 10565-10569. https://doi.org/10.1016/j.matpr.2017.06.421.
Han, R., Li, Y. and van de Lindt, J. (2014), "Seismic risk of base isolated non-ductile reinforced concrete buildings considering uncertainties and mainshock–aftershock sequences", *Struct. Saf.*, **50**, 39-56. https://doi.org/10.1016/j.strusafe.2014.03.010.
Hussain, S., AlHamaydeh, M.H. and Aly, N.E. (2012), "Jakarta's first seismic-isolated building—A 25 story tower", *Proceedings of the 15th World Conference on Earthquake Engineering (15 WCEE)*, Lisbon, Portugal, 24-28 September 2012.
Ibrahim, Y.E. and El-Shami, M.M. (2011), "Seismic fragility curves for mid-rise reinforced concrete frames in Kingdom of Saudi Arabia", *The IES J. Part A: Civil & Struct. Eng.*, **4**(4), 213-223. https://doi.org/10.1080/19373260.2011.609325.
Imran, I., Siringoringo, D.M. and Michael, J. (2021), "Seismic performance of reinforced concrete buildings with double concave friction pendulum base isolation system: Case study of design by Indonesian code", *Structures*, **34**, 462-478. https://doi.org/10.1016/j.istruc.2021.07.084.
Irfan, Z., Abdullah, A. and Afifuddin, M. (2022), "Development of fragility curve based on incremental dynamic analysis curve using ground motion Aceh earthquake", E3S Web of Conferences, **340**, 02001. https://doi.org/10.1051/e3sconf/202234002001.
Irsyam, M., Asrurifak, M., Mikhail, R., Wahdiny, I.I., Rustiani, S. and Munirwansyah, M. (2017a), "Development of nationwide VS30 map and calibrated conversion table for Indonesia using automated topographical classification", *J. Eng. Technol. Sci.*, **49**(4), 457-471. https://doi.org/10.5614/j.eng.technol.sci.2017.49.4.3.
Irsyam, M., Hendriyawan, Natawijaya, D.H., Daryono, M.R., Widiyantoro, S., Asrurifak, M. and Faizal, L. (2017b), "Development of new seismic hazard maps of Indonesia 2017", *Proceedings of the 19th International Conference on Soil Mechanics and Geotechnical Engineering*, Seoul, South Korea. 17-21 September 2017.
Japan Society of Seismic Isolation (JSSI) (2010), Seismic Isolation - from the Basics of Components to Design and Construction (in Japanese). Omusha.
Juliafad, E. (2022), "Seismic fragility function for single storey masonry wall RC Building in Padang City", *Indonesia. Int. J. Geomate*, **22**(94). https://doi.org/10.21660/2022.94.3160.
Kato, H., Nasarafu, T., Ishiyama, Y., Ison, R., Sakuma, J. and Kita, S. (2017), "Comparison studies on structural codes-seismic codes in South East Asia", *Proceedings of the 16th World Conference on Earthquake (16WCEE)*, Santiago, Chile.
Khalfan, M. (2013), Fragility curves for residential buildings in developing countries: as case study on non-engineered unreinforced masonry homes in Bantul, Indonesia. McMaster University.
Kossobokov, V.G. and Nekrasova, A.K. (2018), "Aftershock sequences of the recent major earthquakes in New Zealand", *Pure Appl. Geophys.*, **176**(1), 1-23. https://doi.org/10.1007/s00024-018-2071-y.
Maidiawati, M., Tanjung, J., Sanada, Y., Nugroho, F. and Wardi, S. (2020), "Seismic analysis of damaged buildings based on post-earthquake investigation of the 2018 Palu Earthquake", *Int. J. Geomate*, **18**(70). https://doi.org/10.21660/2020.70.9490.
Miwada, G., Sano, T., Katsumata, H., Takiyama, N., Onishi, Y. and Hayashi, Y. (2012), "Experimental study on hysterisis characteristics of the retaining wall of the base-isolated building", *Proceedings of the 15th World Conference on Earthquake Engineering (15 WCEE)*, Lisbon, Portugal, 24-28 September 2012.
Muntafi, Y., Nojima, N. and Jamal, A.U. (2020), "Damage probability assessment of hospital buildings in

Yogyakarta, Indonesia as essential facility due to an earthquake scenario", *J. Civil Eng. Forum*, **6**(3), 225. https://doi.org/10.22146/jcef.53387.

Nagae, T., Suita, K. and Nakashima, M. (2006), "Performance assessment of reinforced concrete buildings with soft first stories", *Annual of Disaster Prevention Research Institute*, **49**, 189-196. Kyoto University.

National Center for Earthquake Studies (2022), Indonesian deaggregation maps for design and evaluation of seismic resistance infrastructure (in Indonesian). prepared by National Center for Earthquake Studies for Ministry Public Works and Housing of Indonesia.

Nugroho, W.O., Sagara, A. and Imran, I. (2022), "The evolution of Indonesian seismic and concrete building codes: From the past to the present", *Structures*, **41**, 1092-1108. https://doi.org/10.1016/j.istruc.2022.05.032.

Pribadi, K.S., Abduh, M., Wirahadikusumah, R.D., Hanifa, N.R., Irsyam, M., Kusumaningrum, P. and Puri, E. (2021), "Learning from past earthquake disasters: The need for knowledge management system to enhance infrastructure resilience in Indonesia", *Int. J. Disaster Risk Reduction*, **64**, 102424. https://doi.org/10.1016/j.ijdrr.2021.102424.

Qu, Z., Kishiki, S. and Nakazawa, T. (2013), "Influence of isolation gap size on the collapse performance of seismically base-isolated buildings", *Earthq. Spectra*, **29**(4), 1477-1494. https://doi.org/10.1193/031912eqs097m.

Rajkumari, S., Thakkar, K. and Goyal, H. (2022), "Fragility analysis of structures subjected to seismic excitation: A state-of-the-art review", *Structures*, **40**, 303-316. https://doi.org/10.1016/j.istruc.2022.04.023.

Sarli, P.W., Palar, P.S., Azhari, Y., Setiawan, A., Sanjaya, Y., Sharon, S.C. and Imran, I. (2023), "Gaussian process regression for seismic fragility assessment: Application to non-engineered residential buildings in Indonesia", *Buildings*, **13**(1), 59. https://doi.org/10.3390/buildings13010059.

Seki, M. and Lee, J. (2022), "Seismic isolation of the headquartes building of fire service & civil defence (FSCD) in Dhaka City, Bangladesh", *Proceedings of the 3rd European Conference on Earthquake Engineering & Seismology*, Bucharest, Romania, 4-9 September 2022.

SNI 1726:2019 (2019), Indonesia seismic resistance design guideline for buildings and other structures (in Indonesian). National Standardization Agency.

Sukamta, D. (2014), Advances in seismic design and construction in Indonesia. CTBUH 2014 Shanghai Conference Proceedings.

Supendi, P., Ramdhan, M., Priyobudi, Sianipar, D., Wibowo, A., Gunawan, M.T., Rohadi, S. and Elsera, E.M. (2021), "Foreshock–mainshock–aftershock sequence analysis of the January 14 2021 (MW 6.2) Mamuju–Majene (West Sulawesi, Indonesia) earthquake", *Earth, Planets and Space*, **73**(1). https://doi.org/10.1186/s40623-021-01436-x.

Web site: The Center for Engineering Strong Motion Data (CESMD) database website https://www.strongmotioncenter.org/

Web site: The Pacific Earthquake Engineering Research Center (PEER), https://ngawest2.berkeley.edu/site

Xue, Q., Wu, C.W., Chen, C.C. and Chen, K.C. (2008), "The draft code for performance-based seismic design of buildings in Taiwan", *Eng. Struct.*, **30**(6), 1535-1547. https://doi.org/10.1016/j.engstruct.2007.10.002.

Yang, F., Li, C., Wang, T., Liu, D., Yao, S., Li, H., He, J., Huo, Y. and Lei, M. (2023), "Reliability analysis of an inter-story isolated structure under a main-aftershock sequence based on the Laplace asymptotic method", *Front. Earth Sci.*, 11. https://doi.org/10.3389/feart.2023.1121181.

Yenidogan, C. (2021), "Earthquake-resilient design of seismically isolated buildings: A review of technology", *Vibration*, **4**(3), 602-647. https://doi.org/10.3390/vibration4030035.

Zhai, C.H., Zheng, Z., Li, S. and Pan, X. (2016), "Damage accumulation of a base-isolated RCC building under mainshock-aftershock seismic sequences", *KSCE J. Civil Eng.*, **21**(1), 364-377. https://doi.org/10.1007/s12205-016-0701-4.